Time Dependent Hartree-Fock and Beyond

K. GOEKE, R. Y. CUSSON,* F. GRÜMMER,**
P.-G. REINHARD*** and H. REINHARDT****

Institut für Kernphysik, KFA Jülich, D-5170 Jülich
and
Physik-Department, Universität Bonn, D-5300 Bonn
**Department of Physics, Duke University, Durham, North Carolina*
***Institut für Kernphysik, KFA Jülich, D-5170 Jülich*
****Institut für Kernphysik, Universität Mainz, D-6500 Mainz*
*****Zentralinstitut für Kernforschung, Rossendorf, Dresden*

(Received July 30, 1982)

The time dependent Hartree-Fock method (TDHF) is reviewed and its success and failure are discussed following realistic numerical results. It is demonstrated that TDHF is basically able to describe the time evolution of one-body operators, the energy loss in inclusive deep inelastic collisions, and fusion reactions above the Coulomb barrier. For spontaneous fission, subbarrier fusion and the description of bound vibrations the quantized adiabatic time dependent Hartree-Fock theory (quantized ATDHF) is suggested and reviewed. Realistic three-dimensional calculations for heavy ion systems of $A_1+A_2\leq 32$ are presented. Recent theories based on path integral approaches (PIA) are discussed, which aim at quantizing TDHF in order to describe stationary vibrational states and subbarrier fission. The relationship of quantized ATDHF to PIA is explored in the case of vibrations including the fluctuations on top of the periodic TDHF orbits. The above methods to go beyond TDHF concern the quantum mechanical content of TDHF. For the description of width of one-body observables in inclusive reactions the time dependent generator coordinate method (TDGCM) is reviewed. It appears in one-dimensional calculations to be able to enlarge the width obtained in TDHF by an order of magnitude. It is argued that this is because a superposition of mean fields is considered in contrast to other approaches which consider collision terms in a single modified TDHF mean field.

§ 1. Introduction

Over the past two decades there has been a constant activity among nuclear theorists towards a consistent description of large amplitude collective nuclear motion as, e.g., fission and fusion processes, nonharmonic vibrations of soft nuclei, heavy ion reactions, etc. Most of the more conventional approaches aim to reduce the many-body problem by introducing collective coordinates as, e.g., necking and elongation in the fission process, multipole moments in nuclear vibrations, the relative distance between the ions in fusion

processes and heavy ion reactions. In those microscopic-macroscopic theories the connection between single particle motion and collective motion is mediated by a single particle potential the shape of which is chosen on the basis of a preconceived knowledge of the collective motion.

Actually some years ago this concept received a new impulse by the desire not to introduce the collective dynamics by an educated guess but rather to describe the system fully by means of a systematic many-body theory using as input only an effective two-body interaction. This new emphasis has resulted from the suspicion that particularly for large amplitude collective motions one introduces uncontrollable limitations on the dynamics of the system by imposing certain geometrical shapes for the system rather than allowing its free evolution. The first important step in this direction was the formulation and application of the time dependent Hartree-Fock theory[1)~5)] (TDHF).

In spite of the great success of TDHF and the enormous stimulation it has caused, its limitations have become rather apparent and are frequently being discussed in the literature. Its shortcomings consist for instance in a lack of a quantization procedure for the description of discrete bound states, the impossibility of applying TDHF to barrier penetration phenomena and the inadequate implementation of boundary conditions in scattering processes. In addition only one-body operators can be evaluated without providing a good description of their fluctuation, the most important example being the particle number width in deep inelastic collisions. These difficulties gave rise to basically four different theoretical developments to be discussed in this lecture, which all incorporate to some extent elements of TDHF but in the end go conceptually and in the results beyond TDHF.

One group of approaches includes theories like adiabatic TDHF combined with generator coordinate methods.[6)~14)] The second group of theories[15)~18)] comprises path integral approaches (PIA). The third group of theories includes approaches to consider not the time evolution of a Slater determinant but of a more general state incorporating certain RPA correlations.[19),20)] The fourth sort of theories, only roughly sketched in this lecture, includes approaches to go beyond TDHF by the inclusion of some sort of Boltzmann's collision term.[21)~27)] It should be mentioned that more or less all theories described and to be discussed in detail are reviewed in the lectures collected in Ref. 5). In the present lecture we do not discuss the formal details of the theories, but will rather give a general qualitative review with numerical results.

§ 2. TDHF: Success and failure

The TDHF approach assumes the initial condition of a HI reaction, i.e., two undisturbed ions of A_1 and A_2 particles with a certain relative

velocity and a certain impact parameter, to be represented by a Slater determinant of $A=A_1+A_2$ single particle states. If the well separated ions are assumed in their HF ground states, this is certainly a reasonable approximation. The basic assumption of TDHF is now, that the total wave function can for all times be assumed as a Slater determinant $\phi(\boldsymbol{r}_1, \cdots, \boldsymbol{r}_A, t)$. With this assumption the equation of motion for the total system of $A_1+A_2=A$ nucleons is precisely given by the TDHF-equation.

$$i\hbar\frac{\partial}{\partial t}\phi(\boldsymbol{r}_1, \cdots, \boldsymbol{r}_A, t)=\{\sum_{i=1}^{A} h_i[\rho]\}\phi(\boldsymbol{r}_1, \cdots, \boldsymbol{r}_A, t). \tag{2·1}$$

Here $h_i[\rho]$ is the TDHF single particle Hamiltonian depending on the density matrix $\rho^{(+)}$ of the total system:

$$h_i[\rho]=-\frac{\hbar^2}{2m}\nabla_i^2+U[\rho](\boldsymbol{r}_i), \tag{2·2}$$

where $U[\rho](\boldsymbol{r}_i)$ is the mean field including all exchange terms and ρ is given by the single particle wave functions $\varphi_\alpha(\boldsymbol{r}, t)$ as

$$\rho(\boldsymbol{r}, \boldsymbol{r}', t)=\sum_{\alpha=1}^{A}\varphi_\alpha^*(\boldsymbol{r}, t)\varphi_\alpha(\boldsymbol{r}', t). \tag{2·3}$$

Today there is a huge number of numerical solutions of the TDHF equations. They all are done representing the single particle wave functions by their values on a two- or three-dimensional grid in the coordinate space and solving Eq. (2·1) by finite differences in time. The effective two-body interaction, whose average over the time dependent density gives $U[\rho(t)]$, is usually taken to be of Skyrme type. This has the advantage that the exchange terms are local and can therefore be easily handled. The Bonche-Koonin-Negele interaction[1] is also frequently used, it corresponds to the $t_0\sim t_3$-terms in the Skyrme force plus a direct Yukawa term, and sometimes also a direct Coulomb term is added.

The first success of TDHF actually consisted in providing a deep insight into the geometry of nuclear shapes relevant for HI reactions. This was due to the fact that one could perform snapshots of the mass density distribution revealing, e.g., details on neck formation in the entrance and exit channel. However the first experimentally significant data was the fusion cross section of light heavy ions. Here fusion is defined by the sticking together of the ions for more than one or two revolutions, see Fig. 1 as an example. The result for the fusion is given in Fig. 2. One actually realizes a fair agreement of the TDHF with experiment, in particular, if one takes into account that there are no free parameters besides those of the force which itself is determined by reproducing rms-radii and energies all over the periodic table. The second experimental data reproduced by TDHF are the Wilczynski-plots of various

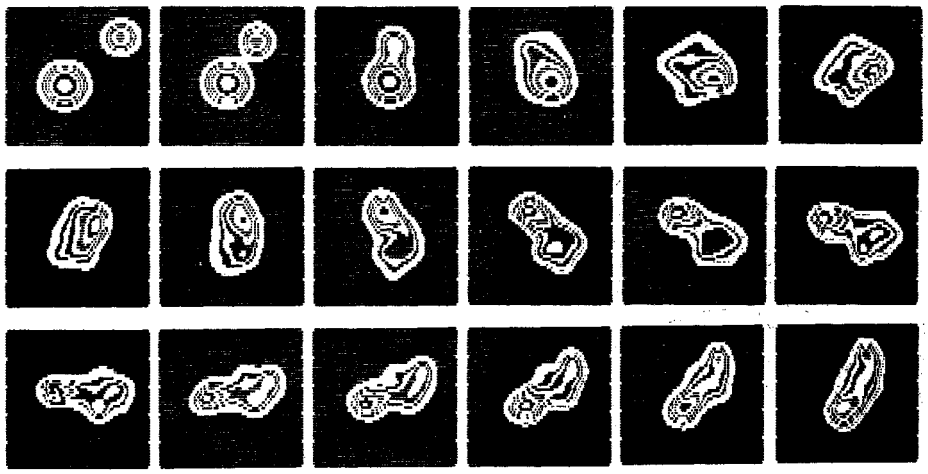

Fig. 1. Contour plot at sequential times for the density in the CM-frame integrated over the normal to the reaction plane for an $^{16}O+^{40}Ca$ collision at a laboratory energy of 315 MeV and an impact parameter corresponding to $l=60\hbar$ initial relative angular momentum. Taken from Ref. 4).

HI reactions, see, e.g., Fig. 3. Here the ridges of the rather complicated mountains of the plot are reasonably well reproduced. This also should be considered as a great success of TDHF, since by now it is the only fully microscopic theory which does this.

From these two points one can learn that TDHF seems to be a suitable theory for the description of the energy flow from the relative motion in the entrance channel to the internal excitations in the outgoing fusion or deep inelastic channel. Furthermore, mean values of one-body operators are also well described as, e.g., the mean particle number in the projectile-like fragment in deep inelastic collisions. The reason for both features lies in the fact that TDHF is just a theory for the propagation of the one-body density matrix and that one uses effective interactions, fitted to experimental data, in particular, rms-radii and energies in a HF framework.

From these considerations one realizes immediately that TDHF will not be able to reproduce the widths of one-body operators, being themselves two-body operators, since the two-body density matrix of TDHF is just a trivial product of the one-body one. Indeed, the width of the particle number distribution of either fragment in a deep inelastic HI event is underestimated in TDHF by an order of magnitude. Precisely this motivates theories which try to incorporate collision terms or which try to propagate RPA correlated states rather than considering only pure Slater determinants.

A second sort of shortcomings concerns the failure of TDHF to describe penetration processes. If the energy of a HI reaction process is less than the height of the Coulomb Barrier, the TDHF describes merely a nearly elastic

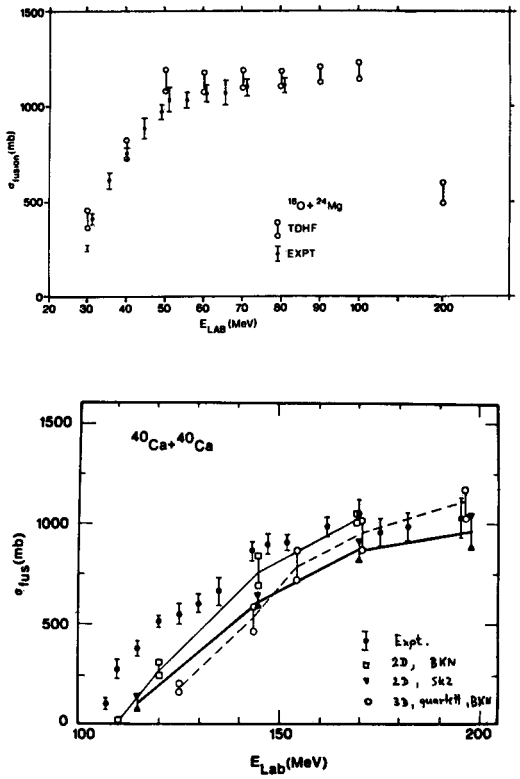

Fig. 2. TDHF calculations for nuclear fusion (above the Coulomb barrier). Taken from Ref. 4).

rebounding of the two ions without giving appreciable tunneling. This is not principally forbidden, but the restriction to a Slater determinant and one common potential to move in simply prevents the tunneling from taking place. Similar things happen if one likes to describe fission under the barrier. In such a case the TDHF solution vibrates inside the potential barrier and does not get out.

A third shortcoming of TDHF lies in the fact that it cannot describe discrete vibrational levels, corresponding to stationary states. If the TDHF solution is moving inside some potential well describing, e.g., the potential energy surface associated to a vibration, then, if at all, it provides periodic solutions for a full continuum of energies. It does not, however, give a prescription which of the energies are to be selected in order to account for the stationary 0-phonon, 1-phonon, etc., states.

A further drawback of TDHF is that one can only give the classical cross section, given by the deflection function, of a HI reaction and not S-matrix elements and phase shifts. This drawback will not be discussed further.

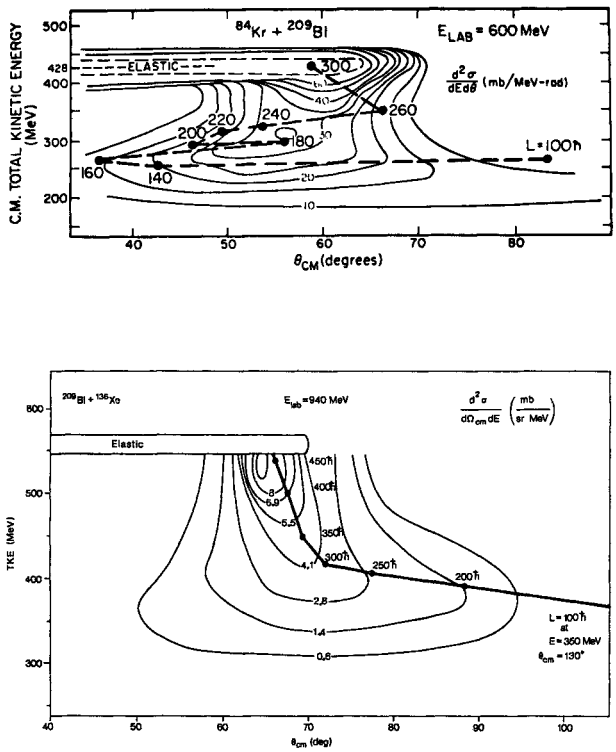

Fig. 3. Wilczynski-plots for $^{84}Kr+^{209}Bi$ and $^{136}Xe+^{209}Bi$ at $E_{LAB}=600$ MeV and 940 MeV, respectively. The calculated points are labelled with the orbital angular momentum. Taken from Ref. 4).

§ 3. Beyond TDHF: Quantized ATDHF

In this section we discuss the possibility to extract from the many-body Hamiltonian of the total $A_1+A_2=A$ system a collective sub-Hamiltonian which describes the degree of freedom associated to the relative motion of the ions. This will then enable us to describe subbarrier fusion, spontaneous fission and bound vibrations and also to some extent phase shifts. The sub-Hilbert-space is assumed to be spanned by a manifold of Slater determinants $|\phi_{R\dot{R}}\rangle$ or $|\phi_{qp}\rangle$ in general. The set of $|\phi_{qp}\rangle$ forms the so-called collective path $\{|\phi_{qp}\rangle\}$. The collective path is supposed to be constructed such that any state $|\psi_n\rangle$ of the collectively moving system without intrinsic excitations is to a good approximation contained in the Hilbert subspace spanned by the path $\{|\phi_{qp}\rangle\}$:

$$|\psi_n\rangle = \int dqdp f_n(q, p)\,|\phi_{qp}\rangle \tag{3·1}$$

with superposition functions $f_n(q, p)$. Actually Eq. (3·1) is some sort of generalized separation ansatz. It decomposes the problem of solving the exact Schrödinger equation in the case of collective motion into three simpler ones: (1) Finding an optimal collective path $\{|\phi_{qp}\rangle\}$ which decouples maximally the collective motion from the internal excitations. (2) Invoking, for the now given path, a quantization procedure which in the end allows to determine the $f_n(q, p)$ and hence the collective wave functions with all their properties. (3) Estimating the coupling of the $|\psi_n\rangle$, thus obtained, to the residual Hilbert-space, thereby giving a measure for the validity of the whole approach in the particular case considered. Actually there are various groups who have suggested solutions to some of the above points.[8)~14)] In this paper we follow the approach of Goeke and Reinhard since it is the only one which includes a validity condition and has been applied in a realistic way, see Refs. 7), 12) ~14) for details. This approach we call quantized ATDHF.

There are two alternative variational principles based on which one can set up rules for performing the above three steps. The one[10)] is the time dependent variational principle of TDHF, and the other[13)] is the stationary variational principle of the generator-coordinate-method (GCM). Both ways have been shown[18)] to lead to exactly the same result. In the following we give a short review of the derivarion by means of the GCM. It is conceptually the simplest, however, technically more involved, thus we do not go into details. We start with the variational principle

$$\delta \int dqdpdq'dp' f^*(q, p)\langle\phi_{qp}|H-E|\phi_{q'p'}\rangle f(q', p') = 0 \qquad (3\cdot2)$$

and have to vary with respect to the path $\langle\phi_{qp}|$ and with respect to the superposition $f^*(q, p)$.

The first point[13)] in quantized ATDHF consists in deriving an equation for the path, the so-called ATDHF equation. To this end we consider the variation with respect to the path using the Gaussian-overlap approximation. The second approximation is an adiabatic expansion about $p=0$ in powers of p, where we consider an adiabatic path up to order p^1 which can be parametrized as

$$|\phi_{qp}\rangle = \exp\{ip\hat{Q}(q)\}|\phi_q\rangle, \qquad (3\cdot3)$$

i.e., it is fixed completely by the knowledge of the first order expansion $|\phi_{qp}\rangle \simeq |\phi_{qp=0}\rangle + ip\hat{Q}(q)|\phi_{qp=0}\rangle$ where $\hat{Q}(q)|\phi_q\rangle = -i\partial_p|\phi_{qp}\rangle|_{p=0}$. As a third point (not really a new approximation), we have to recall that the path is an expansion basis for a series of states in the collective spectrum; thus the path is demanded to be independent of the actual superposition function $f_n(q, p)$. This postulate is consistent with demanding a local and energy independent quantized collective Hamiltonian. Altogether we obtain in order p^0

$$\langle\phi_q|\left[a^\dagger a,\ H-\frac{\partial\mathcal{V}}{\partial q}\hat{Q}\right]|\phi_q\rangle=0 \tag{3·4a}$$

and in order p^1

$$\langle\phi_q|\left[a^\dagger a,\ [H,\hat{Q}]+\frac{i}{\mathcal{M}}\hat{P}\right]|\phi_q\rangle=0, \tag{3·4b}$$

where $a^\dagger a$ can be any 1ph operator and $\hat{P}|\phi_q\rangle=i\partial_q|\phi_q\rangle$. The classical potential is

$$\mathcal{V}(q)=\langle\phi_q|H|\phi_q\rangle \tag{3·5}$$

and the mass parameter is given by

$$\frac{1}{\mathcal{M}(q)}=\langle\phi_q|[\hat{Q},\ [H,\hat{Q}]]|\phi_q\rangle \tag{3·6}$$

with

$$\hat{Q}(q)=\left(\frac{\partial\mathcal{V}}{\partial q}\right)^{-1}H_{\rm ph}(q)\ . \tag{3·7}$$

Equations (3·4) are a coupled system determining (not yet uniquely) $|\phi_q\rangle$ and $\hat{Q}(q)$. They have independently been derived by Villars[9] and Goeke and Reinhard.[10] For a numerical treatment it is essential to realize that they can be recombined to one differential equation for the path[12),14)]

$$\frac{\partial}{\partial q}|\phi_q\rangle=\frac{\mathcal{M}}{\partial\mathcal{V}/\partial q}[H,\ H_{\rm ph}]_{\rm ph}|\phi_q\rangle\ . \tag{3·8}$$

The above formulation is independent of the way in which the parametrization is chosen. For convenience one may introduce a measuring operator D which defines the parameter via $q=\langle\phi_q|D|\phi_q\rangle$.

The second point in quantized ATDHF, viz., the quantization, is now straightforward although technically involved. The variation (3·2) with respect to $f_n^*(q,p)$ yields a generalized Griffin-Hill-Wheeler integral equation for $f_n(q,p)$. With the same two approximations as before, i.e., GOA and adiabatic expansion, one can derive[35)] from it a differential equation of the type of a Schrödinger equation. The fact that one deals with a set of two conjugate parameters, q and p, corresponds to a Peierls-Thouless double projection method and ensures an accurate asymptotic behaviour of the collective mass. One ends up with a collective Hamiltonian[35)]

$$H_c\left(q,\frac{d}{dq}\right)=-\frac{d}{dq}\frac{1}{2\mathcal{M}(q)}\frac{d}{dq}+\mathcal{V}(q)-\mathcal{Z}(q), \tag{3·9}$$

where $\mathcal{M}(q)$ and $\mathcal{V}(q)$ are consistently those of Eq. (3·6) and (3·5).

The $\mathcal{Z}(q)$ include quantum corrections which remove the spurious zero-point energies contained in $\mathcal{V}(q)$ originating from the zero-point motion of the wave packet $|\phi_q\rangle$ along the collective path. They are given by[35]

$$\mathcal{Z}(q)=\frac{1}{2}\langle\phi_q|\hat{Q}^2|\phi_q\rangle\frac{\partial^2\mathcal{V}}{\partial q^2}+\frac{1}{2}\langle\phi_q|\hat{P}^2|\phi_q\rangle\frac{1}{\mathcal{M}}. \tag{3·10}$$

Actually the two basic equations of quantized ATDHF are Eqs. (3·8) and (3·9). As has been shown in Refs. 14) and 28), Eq. (3·8) has not a unique solution but depends, as any first order differential equation, on some initial choice $|\phi_q^{(0)}\rangle$. After that Eq. (3·8) describes simply in the many-dimensional space of Slater determinants a fall line with respect to the metric tensor.[28),29)] A schematic picture for a two level landscape model is given in Fig. 4. Each curve represents a fall line, all of which however converge to the one from the saddle point (marked by $\times$) towards the minimum. This particular fall line is distinguished from the others by the fact that it fulfills best the validity condition

$$(p(q))^2\left\|\frac{\partial Q}{\partial p}\right\|_{p=0}\ll 1 \tag{3·11}$$

with $p^2(q)/2\mathcal{M}=E(\text{saddle})-\mathcal{V}(q)$. As derived in Ref. 12) and discussed in Refs. 28) and 29), the saddlepoint-HF-fall line is a geodesy if the validity condition is fulfilled to zero for all values of the collective coordinate q.

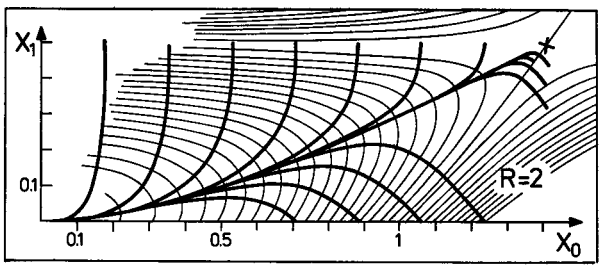

Fig. 4. Schematic picture of the ATDHF fall lines in a two level landscape model. Taken from Ref. 28).

Otherwise (Eq. (3·11)) it is a measure how far the Rowe-Bassermann-Marumori path and the present one differ from each other. If they differ much, then probably both approaches are useless. In practice one proceeds as follows. One solves Eq. (3·8) by the Euler step method, i.e., a neighboured point $|\tilde{\phi}\rangle$ is calculated outgoing from $|\phi\rangle$ by

$$|\tilde{\phi}\rangle=\{1-\varepsilon[H,H_{\text{ph}}(\phi)]_{\text{ph}}\}|\phi\rangle. \tag{3·12}$$

Successive application gives a set of Slater determinants which are afterwards

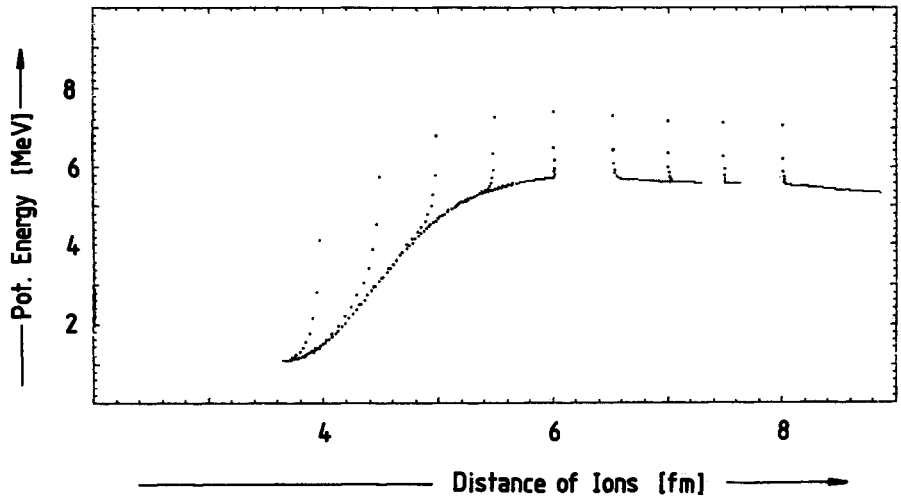

Fig. 5. Solutions of the ATDHF equations (3·8, 3·12) of Goeke and Reinhard starting from initial α-α configurations with various distances of the fragments.

labelled by the distance R of the ions obtained from the total quadrupole moments $\langle Q\rangle\langle Q\rangle = 1/2 \cdot AR^2 + \langle Q_1\rangle + \langle Q_2\rangle$ where $\langle Q_i\rangle$ are the quadrupole moments of the fragments. Figure 5 illustrates how one finds the saddle point and how the various fall lines converge to the collective path (i.e., the saddle-HF-fall line). The calculations are performed using a BKN-force plus Coulomb interaction representing the single particle wave functions by a 16 $\times 16 \times 24$ mesh of 1 fm gridsize. The ε must be smaller than $10^{-4}\,\mathrm{MeV}^{-2}$ in order to obtain stable solutions of Eq. (3·12). Each dot in Fig. 5 is the result of ten steps (3·12). The initial solutions have been chosen to be $\alpha-\alpha$ configurations with an R value ranging from $R=4$ fm to $R=8$ fm. One notices the saddle point at $R=6.2$ fm and the HF-^{8}Be-point at $R=3.4$ fm. One realizes that the single dots accumulate to a clear line representing the potential $\mathcal{V}(R) = \langle \phi_R | H | \phi_R \rangle$ for all R values greater than the R-value at the ^{8}Be-HF point. The final results of the $\alpha + \alpha \leftrightarrow {}^8$Be system are given in Fig. 6, where the classical potential, $\mathcal{V}(R)$, the quantum corrected, $\mathcal{V}(R) - \mathcal{Z}(R)$, and the mass parameter are plotted. One realizes that the mass parameter approaches the correct asymptotic value. The zero point energies $\mathcal{Z}(R)$ are plotted in Fig. 7. They originate from spurious rotation of the total system, spurious center-of-mass motion of the total system in x- and z-direction and spurious relative motion of the fragments. The total $\mathcal{Z}(R)$ is a rather smooth curve.

Figure 8(a) and (b) show some density distributions occuring in the ^{16}O $+ {}^{16}\mathrm{O} \leftrightarrow {}^{32}$S process and Fig. 9 cuts through the densities along the axis connecting the two fragments. One realizes the buildup of a small density increase at $R=6.6$ fm before the density relaxes to its HF-^{32}S-value. The

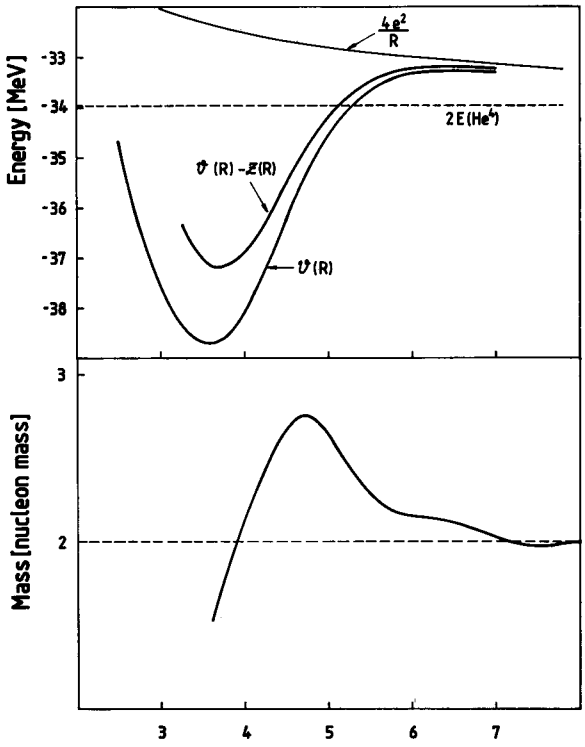

Fig. 6. The classical potential, $\mathcal{V}(R)$, the quantum corrected one, $\mathcal{V}(R)-\mathcal{Z}(R)$, and the mass parameter, $\mathcal{M}(R)$, versus the distance R of the ions for the $\alpha+\alpha\leftrightarrow{}^8$Be system. All quantities are calculated by the quantized ATDHF approach.

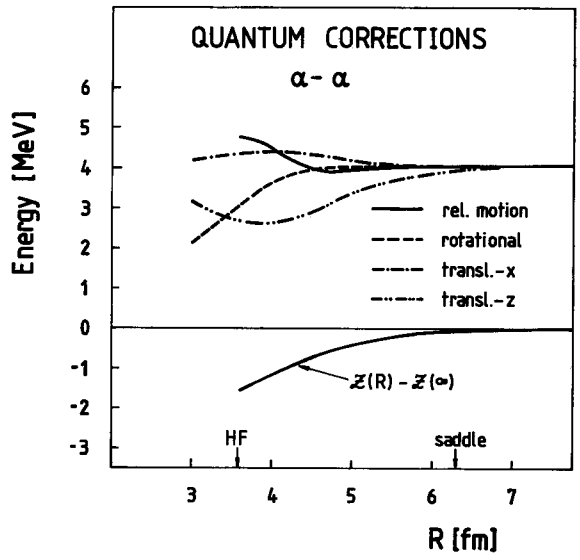

Fig. 7. The quantum corrections of the $\alpha+\alpha\leftrightarrow{}^8$Be system versus the distance of the α-fragments, calculated by quantized ATDHF.

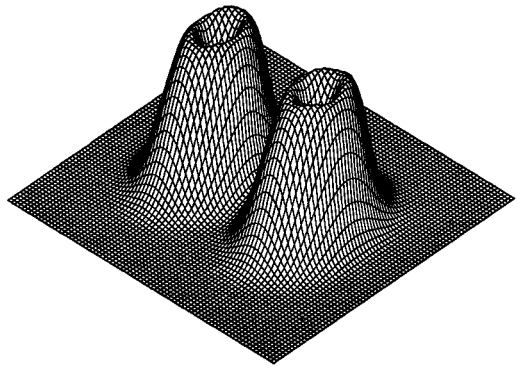

(a)

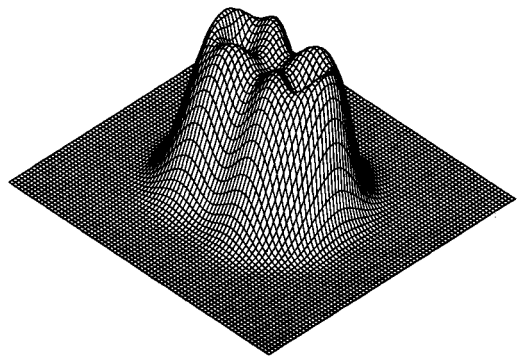

(b)

Fig. 8. Density plots for the $^{16}O + ^{16}O \leftrightarrow ^{32}S$ collision at two distances close to the saddle point and close to the ^{32}S-HF value, calculated by quantized ATDHF.

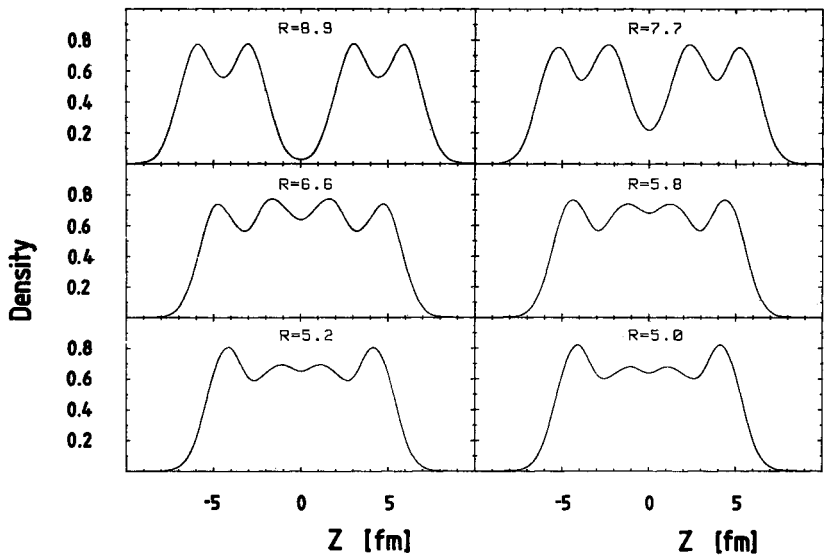

Fig. 9. A cut through the density distribution of the $^{16}O + ^{16}O \leftrightarrow ^{32}S$ reaction at various distances of the ions calculated by quantized ATDHF.

corresponding collective potential and the mass parameter are given in Fig. 10. The potentials are renormalized such that they exhibit the Coulomb tail in the asymptotic region. The mass parameter shows two bumps close to the saddle point and close to the HF point. The quantum corrections look qualitatively similar to the $\alpha+\alpha\leftrightarrow{}^{8}$Be case and are given in Fig. 11. If one inserts all these quantities into the collective Hamiltonian, one is able to evaluate the fusion cross section for events below the Coulomb barrier. The cross

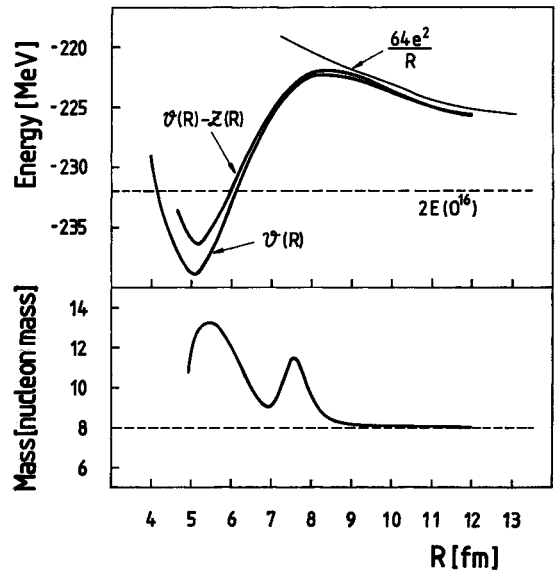

Fig. 10. The classical potential, $\mathcal{V}(R)$, the quantum corrected, $\mathcal{V}(R)-\mathcal{Z}(R)$, and the mass parameter of the $^{16}O+^{16}O\leftrightarrow{}^{32}S$ reaction, calculated by quantized ATDHF.

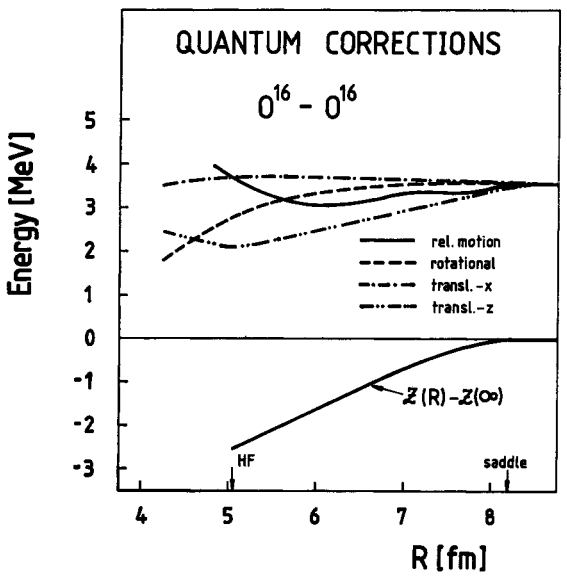

Fig. 11. The quantum corrections of the $^{16}O+^{16}O\leftrightarrow{}^{32}S$ system, calculated by quantized ATDHF.

section is given by

$$\sigma_{\mathrm{fus}}(E_{\mathrm{CM}}) = \lambda^2 \sum_L (2L+1)\, T_L(E_{\mathrm{CM}}) \tag{3·13}$$

and the transmission coefficients are

$$T_L = \exp\left[-2\int_a^b \left\{\frac{2\mathcal{M}(R)}{\hbar^2}\left[\mathcal{V}(R) - \mathcal{Z}(R) + \frac{\hbar^2}{2\Theta(R)}L(L+1) - E_{\mathrm{CM}}\right]\right\}^{1/2} dR\right], \tag{3·14}$$

where a and b are the classical turning points. For the $^{16}O+^{16}O \leftrightarrow ^{32}S$ reaction the fusion cross section is given in Fig. 12 and the corresponding astrophysical S-factor in Fig. 13. One realizes that the fusion cross section is qualitatively reproduced, however, there is a factor $2\sim5$ missing and, as one sees in Fig. 13, also the slope is slightly wrong. Since fusion reactions above the barrier are better reproduced by TDHF with the BKN force, it seems to be that the subbarrier cross sections are much more sensitive to the details of the force

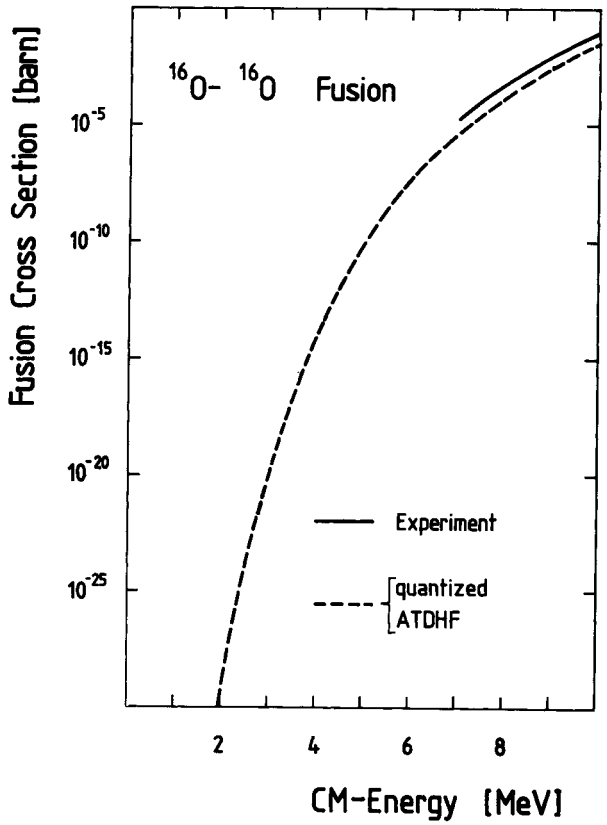

Fig. 12. Subbarrier fusion cross section for the $^{16}O+^{16}O \leftrightarrow ^{32}S$ reaction. The solid line represents the experiment, the dashed line is quantized ATDHF.

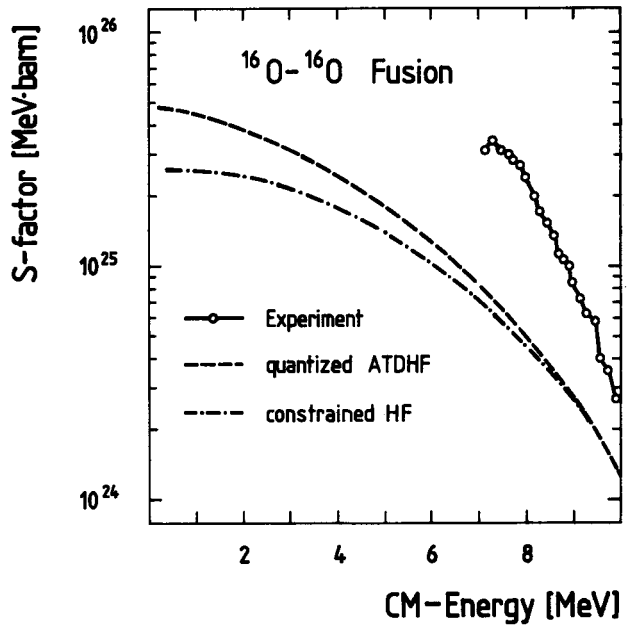

Fig. 13. The astorophysical S-factor of the $^{16}O+^{16}O \leftrightarrow ^{32}S$ subbarrier fusion event. Given are experimental data and the results of quantized ATDHF and constrained HF with the quadrupole moment as constraining force. The CHF data are taken from Ref. 30).

than superbarrier ones.

We have also studied the $^{12}C+^{12}C \leftrightarrow ^{24}Mg$ reaction. Actually with the present symmetries there are basically two initial conditions possible; an axial symmetric configuration, where the two flat ions are parallel, and a triaxial one, where the two flat ions lie in a plane. All other possible configurations are probably some sort of average between these two. Figures 14 and 15 show the respective mass parameters and potentials. As is expected, the saddlepoint of the triaxial solution lies at a noticeably larger distance than that of the axial solution. The corresponding HF-^{24}Mg-minimum is less deep. The fact that we have for each asymptotic configuration an own HF minimum is due to the symmetry restrictions imposed on the single particle wave functions. It will be a task in the near future to release these restrictions and to reinvestigate then the $^{12}C+^{12}C \leftrightarrow ^{24}Mg$ system.

It is interesting to compare the collective path obtained by the present ATDHF method with the one obtained by means of constrained Hartree-Fock (CHF). The standard choice for the constraint in the present systems is the quadrupole operator. Flocard et al.[30] have done calculations for the $^{16}O+^{16}O \leftrightarrow ^{32}S$ and the $^{12}C+^{12}C \leftrightarrow ^{24}Mg$ system. Besides the method used the technicalities of the calculations were similar to the ones used here. Thus the results are directly comparable. Whereas the potentials are not much different the mass

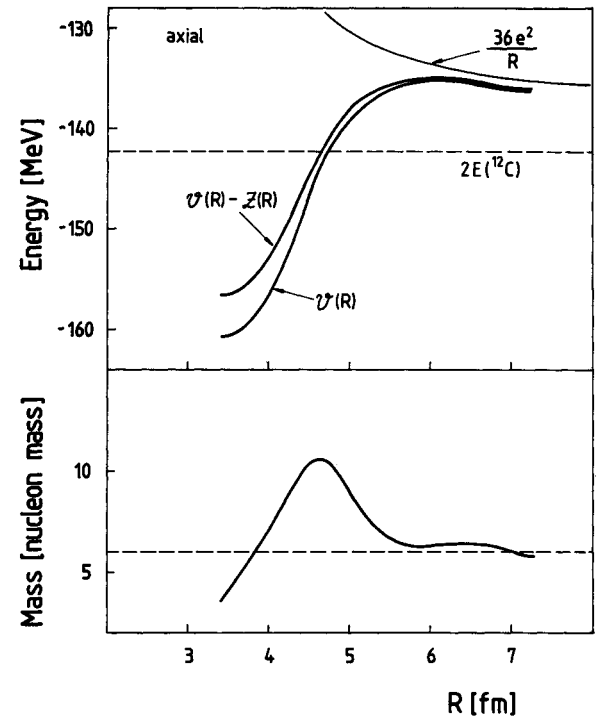

Fig. 14. The classical potential, $\mathcal{V}(R)$, the quantum corrected, $\mathcal{V}(R)-\mathcal{Z}(R)$, and the mass parameter of the $^{12}C+^{12}C\leftrightarrow^{24}Mg$ system assuming axial symmetry, calculated by quantized ATDHF.

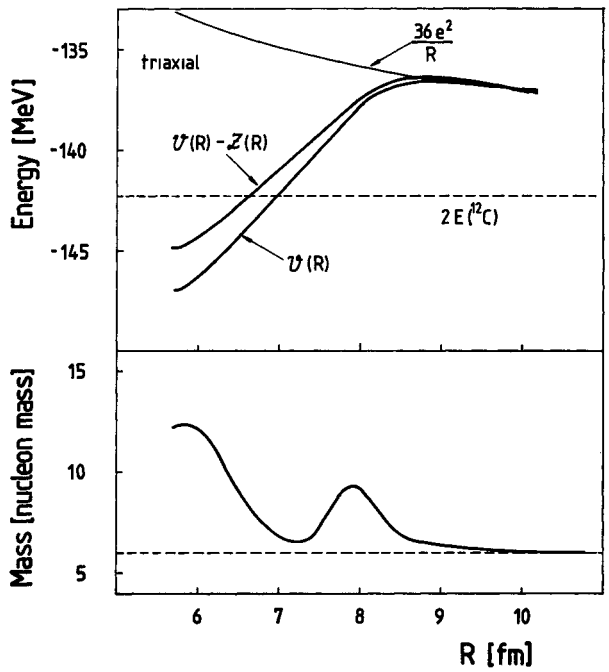

Fig. 15. The same as Fig. 14, but with a triaxial configuration. Calculated by quantized ATDHF.

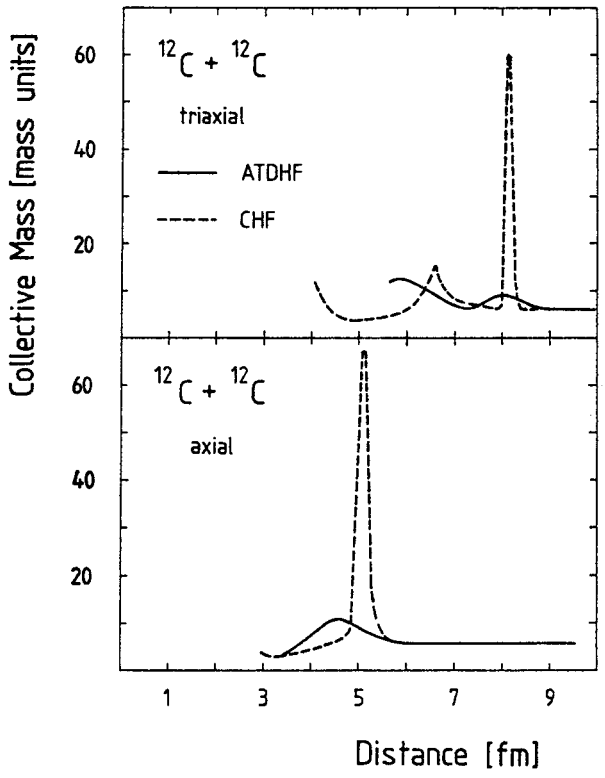

Fig. 16. The mass parameter of quantized ATDHF and of CHF evaluated for the system $^{12}C+^{12}C \leftrightarrow ^{24}Mg$.

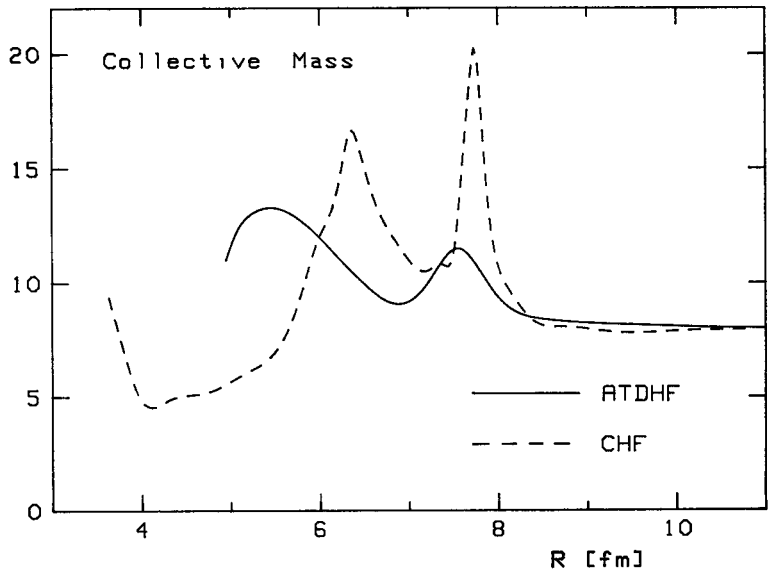

Fig. 17. The mass parameter of quantized ATDHF and of CHF evaluated for the $^{16}O+^{16}O \leftrightarrow ^{32}S$ system.

parameters turn out to be quite sensitive to the path used, CHF or ATDHF. This can be seen in Figs. 16 and 17. Apparently, as far as the mass is concerned, the CHF is not a good approximation to ATDHF. The spikes and sharp peaks of the CHF-masses seem to be an artificial property of the CHF-method. One can conclude this section on quantized ATDHF:

The present numbers are the first ones which come out for ATDHF in a realistic situation. They demonstrate that ATDHF, at least in the way formulated by Goeke and Reinhard, is numerically applicable and yields a unique solution. Since in this framework quantization processes are well understood without any problems, one has a versatile tool to extract the maximally decoupled collective Hamiltonian for a nuclear system.

§ 4. Beyond TDHF: Path integral approaches

The basic feature of the path integral theory is that it expresses the time evolution of a many-body system, subjected to two-body interactions, by a coherent sum over the time evolution of the system in mean fields. Actually, one considers the multitude of (classical) trajectories of the system in all possible external one-body potentials (mean fields) and performs a functional integral over them with the weight given in terms of the two-body interaction. Of particular interest are those trajectories which satisfy the stationary phase condition since in many circumstances they dominate the time evolutions of the mean field. The actual conditions depend on the matrix element of the time evolution operator associated to the motion under consideration.

Actually in this formalism there has recently been suggested a mean field theory for nuclear reactions, see, e.g., H. Reinhardt in Ref. 5). In the present lecture we concentrate, however, on the problem of quantizing TDHF in case of stationary vibrations.[15)~18)]

The proper object to study the stationary properties of a self bound system is the partition function, i.e., the trace of the time evolution operator over the complete space of the system

$$Z^{(T)} = \mathrm{Tr}\{\exp(-i\hat{H}T)\}, \tag{4·1}$$

where H is the microscopic Hamiltonian of the many-body system consisting of a single particle term and the effective two-body interaction V. If $Z^{(T)}$ is known, the basic properties of the system can be extracted. For instance, the exact eigenenergies for stationary motion are given by the poles of the Fourier-transform $\tilde{Z}$ of the partition function:

$$\tilde{Z}(E) = -i\int_0^\infty dT Z^{(T)} e^{tET} = \sum_n \frac{1}{E-E_n}. \tag{4·2}$$

In the approach of Reinhardt[15)] one proceeds by expressing the $Z^{(T)}$ as a

functional integral over all possible density matrices being periodic with period T, i.e., $\rho(t+T)=\rho(t)$. This reads

$$Z^{(T)}=(\mathrm{Det}\,V)^{1/2}\int D\rho\exp\{iS[\rho]\}. \tag{4·3}$$

The $\mathrm{Det}\,V$ is the determinant of the two-body interaction in the configuration time space. The $S[\rho]$ is the action corresponding to $\rho(t)$ and is given by

$$S[\rho]=\frac{1}{2}\int_0^T dt\,\mathrm{Tr}\{\rho(t)V\rho(t)\}-\sum_\nu n_\nu\varepsilon_\nu[\rho]T\,. \tag{4·4}$$

Here the n_ν and $\varepsilon_\nu(T)$ are occupation numbers and Floquet indices of certain single particle states $|f_\nu(t)\rangle$. These are related to $\rho(t)$ by means of the eigenvalue equation

$$\left(i\frac{\partial}{\partial t}-h[\rho]\right)|f_\nu(t)\rangle=-\varepsilon_\nu[\rho]|f_\nu(t)\rangle\,, \tag{4·5}$$

where $h[\rho]$ is the single particle Hamiltonian associated to $\rho(t)$,

$$h[\rho]=\hat{T}+\mathrm{Tr}\{V\rho(t)\} \tag{4·6}$$

and $|f_\nu(t)\rangle$ has the same periodicity as $\rho(t)$:

$$|f_\nu(t)\rangle=|f_\nu(t+T)\rangle. \tag{4·7}$$

Eqs. (4·3)$\sim$(4·7) form a complete system and an exact description of the full partition function.

The virtue of the present PIA consists now in providing in a natural way a semiclassical approximation to the exact functional integral. Such an approximation is expected to be useful for systems performing a large amplitude collective motion because one expects the action $S[\rho]$ to change rapidly (in comparison to the magnitude of $\hbar$) for small changes in the classical trajectories $\rho(t)$. Thus a stationary phase approximation to the integral (4·3) seems to be appropriate, which selects out of the multitude of trajectories $\rho(t)$ those which minimize the action. These particular trajectories can be shown to fulfill the self-consistency condition in addition to Eqs. (4·5)$\sim$(4·7):

$$\rho(t)=\sum_\nu|f_\nu(t)\rangle n_\nu\langle f_\nu(t)|\,. \tag{4·8}$$

The total set of Eqs. (4·5)$\sim$(4·8) is equivalent to a time dependent Hartree-Fock approach (TDHF) with periodic trajectories:

$$\begin{aligned}&i\frac{\partial}{\partial t}\rho(t)=[h[\rho],\rho],\\&\rho(t+T)=\rho(t).\end{aligned} \tag{4·9}$$

For a given period T the total energy of the system is thus constant and can be evaluated as

$$E(T)=\mathrm{Tr}\{\rho\hat{T}\}+\frac{1}{2}\mathrm{TrTr}\{\rho V\rho\}. \tag{4·10}$$

In order to obtain quantized stationary states one has to select from the multitude of periodic TDHF orbits with varying E those which correspond to the poles of the Fourier-transform $\tilde{Z}(E)$ of $Z^{(T)}$. They are distinguished by the fact that the classical action satisfies the condition

$$S(T)-T\frac{\partial}{\partial T}S(T)=2\pi n,\quad n=0,1,2,\cdots \tag{4·11}$$

or explicitly

$$\int_0^T dt\sum_\nu n_\nu\langle f_\nu(t)|i\frac{\partial}{\partial t}|f_\nu(t)\rangle=2\pi n\,. \tag{4·12}$$

This prescription selects some energies E_n corresponding to the stationary states of the system. Actually Griffin et al.[31] have come to the same quantization condition in a different approach.

The above approach can be improved[15] by going beyond TDHF including higher order quantum corrections to the periodic trajectories and thereby to the action, which will eventually lead to a modified quantization rule. To this end we consider small perturbations of the TDHF trajectory, $\rho(t)\to\rho(t)+\varphi(t)$. The time-evolution of the system after perturbation shall again be given by the TDHF equation, starting at time t_0 with $\rho(t_0)+\varphi(t_0)$ instead of $\rho(t_0)$,

$$i\partial_t(\rho+\varphi)=[h(\rho+\varphi),\rho+\varphi]\,. \tag{4·13}$$

If the trajectory $\rho(t)$ is stable, the system will remain close to $\rho(t)$ all time, i.e., $\varphi(t)$ will remain small all time $t>t_0$. We can therefore linearize Eq. (4·13) with respect to the small fluctuations $\varphi(t)$. This yields the so-called linearized stability equation

$$i\partial_t\varphi=L(\rho)\varphi\,, \tag{4·14}$$

where

$$L(\rho)=[h(\rho),\varphi]+[\mathrm{Tr}\,V\varphi,\rho]\,. \tag{4·15}$$

The $L(\rho)$ depends on time via $\rho(t)$ and is also periodic with period T. Therefore, $L(\rho)$ has a complete spectrum of periodic solutions which obey the eigenvalue equation

$$(i\partial_t-L(\rho))\chi_k=-\omega_k\chi_k\,, \tag{4·16}$$

$$\chi_k(t+T)=\chi_k(t)\ , \tag{4·17}$$

where the eigenvalue ω_k is defined up to multiples of $2\pi/T$. For further details see § 6 and Ref. 17). The solutions of the initial value problem Eq. (4·14) can be expressed by the $\chi_k(t)$, i.e.,

$$\varphi(t)=\sum_k c_k \exp(-i\omega_k t)\chi_k(t), \tag{4·18}$$

where the c_k are determined at $\varphi(t=t_0)$.

In order to derive the corrections to the quantization rule one replaces ρ in $S[\rho]$ of Eq. (4·4) by $\rho+\varphi$, changes the integration from $D\rho$ to $D\varphi$ and expands up to φ^2. Then one can evaluate the functional integration over the fluctuating field, being Gaussian in this order, and obtains the corrections expressed in terms of the $f_\nu(t)$ and $\chi_\nu(t)$. One has still the condition (4·11) but due to $\rho\to\rho+\varphi$ with a modified action $S+\Delta S$

$$(S+\Delta S)(T)=\int_0^T dtS(\rho(t))+\frac{1}{2}\sum_{k\neq 0}\omega_k T-\frac{1}{2}\sum_{\text{ph}}(\varepsilon_p-\varepsilon_h)T, \tag{4·19}$$

where $k\neq 0$ excludes the spurious mode from the summation. The spurious mode is the solution of Eq. (4·14) which merely shifts $\rho(t)$ in time, i.e., $\rho(t)+\varphi(t)\simeq\rho(t+\delta t)\simeq\rho(t)+\dot{\rho}(t)\delta t$. It feels no restoring force; therefore, it has $\omega_k=0$ and can get any amplitude.

The meaning of this correction becomes obvious if we evaluate the analogous correction in order $\hbar^2$ to the energy of the system

$$\begin{aligned}(E+\Delta E)(T)=&\operatorname{tr}\{T\rho\}\\&+\frac{1}{2}\operatorname{tr}(\rho V\rho)+\frac{1}{2}\sum_k\frac{1}{T}\int_0^T dt\langle\chi_k|L(\rho)|\chi_k\rangle\\&-\frac{1}{2}\sum_{\text{ph}}\frac{1}{T}\int_0^T dt[\langle f_p|h(\rho)|f_p\rangle-\langle f_h|h(\rho)|f_h\rangle],\end{aligned} \tag{4·20}$$

where $\langle\chi_k|L(\rho)|\chi_k\rangle$ is a shorthand for $\operatorname{tr}\{\chi_k^\dagger[L(\rho),\chi_k]\}$. The first two terms are the Hartree-Fock energy and the third and fourth terms are the correction. Obviously the third term adds the zero-point energies of all the fluctuation modes and the fourth term subtracts the analogous zero-point energies of all the 1p-1h modes. That is precisely the generalization of the correlation energy, well known in stationary RPA theory. Thus the functional integral over the fluctuation φ, expanded up to second order in φ, produces a correlated ground state in the sense of RPA.

Concerning the quantization of TDHF, the results of PIA can be summarized on a two step procedure:

i) Search periodic TDHF solutions for a range of periods T and corresponding energies E.

ii) Select particular energies E_n by the quantization condition. Actual numerical calculations in realistic cases have not yet been established. It is even not known whether periodic TDHF solutions indeed exist at all. To judge the method it might therefore be useful to establish a connection to quantized ATDHF, which is known to be numerically applicable and indeed has very similar objectives on PIA. In fact this connection has recently been discussed in Ref. 32). Without going into details the results can be reviewed as follows:

The path-integral-approach (PIA) considers a multitude of TDHF solutions $\phi_T(t)$, the density matrix of which is periodic with the period T, i.e., $\rho(t+T)=\rho(t)$. Actually there may be various distinct solutions for a given period T being associated, e.g., to different multipole vibrations. However we assume in the following that these different solutions have clearly different characteristics such that one can always identify those associated to the mode one is interested in. We furthermore assume that within certain limits there exists for any T a $\phi_T(t)$ associated to the considered mode and that they are continuously connected. This means that the trajectory $\phi_{T+\delta T}(t)$ is infinitesimally close to $\phi_T(t)$ if δT is small enough. The multitude $\{|\phi_T(t)\rangle\}$ of those solutions (associated to a certain collective mode) we shall call a *branch*. We will assume that a branch contains a HF point and that all quantities calculated from $\phi_T(t)$ will be distinguishable in T and also distinguishable in the energy $E=\langle\phi_T(t)|H|\phi_T(t)\rangle$ and that there is a unique relation between E and T. Hence any Slater determinant, which is a member of a branch, is uniquely characterized by giving E and t, i.e., $|\phi_E(t)\rangle$. This labelling in E and t, rather than in T and t, has the advantage that the energy provides a much more sensitive discrimination, ranging from E_{HF} to the upper end of the branch, whereas T is compressed at $T_{\min}=\omega_{\mathrm{RPA}}^{-1}$ at the lower end of the spectrum (harmonic limit).

Furthermore, this labelling has the convenience that E and t are something like canonically conjugate quantities. This establishes immediately a bridge between a *branch* $\{|\phi_E(t)\rangle\}$ and a *path* $\{|\phi_{qp}\rangle\}$ since both multitudes are characterized by two real parameters which can be understood as classical canonical conjugate variables. Within the branch $\{|\phi_E(t)\rangle\}$ a periodic trajectory $|\phi_E(t)\rangle$ represents an actual classical motion. This is characterized within the path $\{|\phi_{qp}\rangle\}$ by $q=q(t,E)$ and $p=p(t,E)$ which obey the classical equations of motion. Hence the members of a branch and of a path can be related by

$$|\phi_E(t)\rangle\propto|\phi_{q(E,t),p(E,t)}\rangle \tag{4·21}$$

with a reverse relation $E=E(q,p)$ and $t=t(q,p)$ such that $\{|\phi_{qp}\rangle\}$ has the characteristics of a collective path, with canonical labelling, i.e.,

$$\langle\phi_{qp}|\overleftarrow{\partial}_q\vec{\partial}_p-\overleftarrow{\partial}_p\vec{\partial}_q|\phi_{qp}\rangle=i\,. \tag{4·22}$$

We do not prove the existence of such a transformation but assume it. In practice it may be constructed explicitly such that $q(t)$ and $p(t)$ obey classical canonical equations.

In order to establish a connection of a branch to an *adiabatic* path one has first to transform from (q, p) to a new (q', p') such that the trajectories $|\phi_E(t)\rangle$ correspond to $q'(E, t)$ and $p'(E, t)$ which show turning points, i.e., which have two times t_a and t_b at which $p'(E, t_a) = p'(E, t_b) = 0$ (see Fig. 1). We furthermore assume that the states $|\phi^{\mathrm{PIA}}_{q', p'=0}\rangle = |\phi^{\mathrm{PIA}}_{q'}\rangle$ are time even, which simplifies the calculational techniques. Actually the path $\{|\phi_{q'p'}\rangle\}$ is fully identical to $\{|\phi_E(t)\rangle\}$ and it may have any complicated q'- and p'-dependence. An *adiabatic* collective path, however, as it is used in ATDHF, is assumed to have the special structure of a separation ansatz (we omit henceforth the primes at the coordinates q' and p')

$$|\phi^{\mathrm{ATDHF}}_{qp}\rangle = \exp[ipQ(q)^{\mathrm{ATDHF}}]|\phi_q{}^{\mathrm{ATDHF}}\rangle, \tag{4·23}$$

where $Q^{\mathrm{ATDHF}}(q)$ is a 1p-1h operator with respect to $|\phi_q{}^{\mathrm{ATDHF}}\rangle$ corresponding of course to the derivative with respect to p at $p=0$

$$Q^{\mathrm{ATDHF}}(q)|\phi_q{}^{\mathrm{ATDHF}}\rangle = \left(i\frac{\partial}{\partial p}\right)_{\mathrm{1p\text{-}1h}} |\phi^{\mathrm{ATDHF}}_{qp}\rangle_{p=0}. \tag{4·24}$$

Apparently an adiabatic $\{|\phi^{\mathrm{ATDHF}}_{qp}\rangle\}$ is a useful object if it can be constructed in such a way that it is as close as possible to the $\{|\phi^{\mathrm{PIA}}_{qp}\rangle\}$.

If one requires that $|\phi^{\mathrm{PIA}}_{qp}\rangle = (1+ipQ^{\mathrm{PIA}}+\cdots)|\phi^{\mathrm{PIA}}_q\rangle$ and $|\phi^{\mathrm{ATDHF}}_{qp}\rangle = (1+ipQ^{\mathrm{ATDHF}}+\cdots)|\phi^{\mathrm{ATDHF}}_q\rangle$ are identical to order p^1, one obtains exactly the ATDHF equation (3·4a, 3·4b) or equivalently (3·8). It is remarkable that there is such a strong connection between PIA and ATDHF. One also can derive the ATDHF-validity condition from PIA by requiring the deviation between $|\phi^{\mathrm{PIA}}_{qp}\rangle$ and $|\phi^{\mathrm{ATDHF}}_{qp}\rangle$ to be as small as possible in order p^2. For details see Ref. 35).

Concerning the quantization one can proceed as follows. The classical action along the periodic TDHF trajectories is then given by Eq. (4·11) with

$$S(T) = \int_0^T dt \langle \phi_{E(T)}(t)|i\partial_t - \hat{H}|\phi_{E(T)}(t)\rangle. \tag{4·25}$$

If we transform this to $q(t)$ and $p(t)$, we obtain after some algebra

$$S(T) = \int_0^T dt\,(\dot{q}(t)\,p(t) - \mathcal{H}(q(t), p(t))) \tag{4·26}$$

with q and p obeying classical canonical equations with $\mathcal{H}(q, p)$ as classical Hamiltonian.

This is just the semiclassical quantization rule for a system whose dynamics is governed by a Hamiltonian $\mathcal{H}(q, p)$. In the adiabatic limit we expand

$$\mathcal{H}(q, p) = \frac{p^2}{2\mathcal{M}(q)} + \mathcal{V}(q). \tag{4·27}$$

Thus we see that the quantization in PIA at that level involves a Hamiltonian $\mathcal{H}(q, p)$, which is the classical limit of the quantum mechanical Hamiltonian $H_c(q, (d/dq))$ of the quantized ATDHF approach if one ignores the quantum corrections $\mathcal{Z}(q)$ of Eq. (3·9), which is consistent in a strict classical limit. Thus we obtain the satisfying result that a semiclassical quantization of the collective ATDHF-Hamiltonian yields precisely the quantization condition of PIA in the adiabatic limit, if in both theories the quantum corrections are neglected.

If one considers the fluctuations in PIA, a lengthy calculation shows that the action S is changed to

$$S + \Delta S = \int_0^T dt\,(\dot{q}(t)\,p(t) - \tilde{\mathcal{H}}(q(t), p(t))), \tag{4·28}$$

where

$$\tilde{\mathcal{H}}(q, p) = \mathcal{H}(q, p) - \mathcal{Z}^{\mathrm{PIA}}(q) \tag{4·29}$$

with

$$\mathcal{Z}^{\mathrm{PIA}}(q) = \frac{\lambda_0(q)}{4\mathcal{M}_0(q)} + \frac{\partial^2 \mathcal{V}_0(q)}{\partial q^2} \cdot (4\lambda_0(q))^{-1}. \tag{4·30}$$

The PIA expression differs from the corresponding one of quantized ATDHF in that it is lacking the residual two-body interaction in Eq. (4·30) which however is not expected to be a severe limitation.

In summary one can conclude: There is a remarkably close connection between the PIA and quantized ATDHF: If one extracts an adiabatic collective path from the periodic PIA orbits, one obtains exactly the adiabatic TDHF equations derived by Villars[9] and Goeke and Reinhard[10),18)] described in § 3 of this article. If one solves the ATDHF collective Hamiltonian by semiclassical WKB methods, one obtains basically the PIA quantization. These features might perhaps help to solve PIA numerically. It will then be very interesting to see how large the implication of the adiabaticity assumptions are in actual realistic situations. These relationships shed also an interesting light on ATDHF: The ATDHF path appears to be an approximation to a very special *multitude* of TDHF trajectories with *varying energies*, namely, the periodic TDHF orbits. In this context it is interesting to note that no one has actually found yet the periodic TDHF solutions, whereas ATDHF is known to be solvable in realistic cases.

§ 5. Beyond TDHF: Time dependent generator coordinate method

If one considers deep inelastic collisions and the associated quantities evaluated by means of TDHF, one realizes, e.g., that TDHF describes well the mean value of the particle number distribution of, e.g., the projectile-like fragment. The width of the distribution, however, is by an order of magnitude too small in TDHF.

Two different effects are believed to contribute to the large spreading widths. The first one is of a statistical nature and involves random coupling of the collective degrees of freedom of the system to the intrinsic ones. Many different approaches have been developed.[21)~27)] It has not yet explicitly been demonstrated if these theories indeed give an increase of the width compared to TDHF or not. In fact there are arguments[33),34)] that one single particle potential alone hinders the system to develop a large spreading width. Hence a superposition of several time dependent mean fields would be preferable since this is expected to have a large effect on the two-body density matrix.

It is the aim of this section to pursue the approach of calculating RPA-like correlations as a function of time into a heavy ion reaction. To this end we shall proceed from a time dependent generalization of the generator-coordinate variational principle (TDGCM). In the representation of TDGCM we have for the wave function of the total system

$$|\psi(t)\rangle = \int dq f(q, t) |\phi_q(t)\rangle , \tag{5·1}$$

where $|\phi_q(t)\rangle$ represents the collectively distorted time dependent Slater determinants and $f(q, t)$ is the time dependent superposition function. The q is a collective variable associated to the mode whose zero point correlations are under consideration. The assumptions required in order that the deformed single Slater determinants $|\phi_q(t)\rangle$ obey the TDHF equations are made very transparent in the TDGCM. They are basically the Gaussian overlap assumption characteristic of most GCM models, and the neglect of the feedback of the correlations on the Slater determinant equations of motion. We note that the TDHF mean path is itself a large amplitude (semi-classical) time dependent collective path and that we are looking for correlations in collective motions which are orthogonal to the path. We will see that the TDGCM takes into account the effect of the full history of the mean path onto the correlations. We want to point out that this is something very different from a local RPA around the TDHF state at each time separately. In TDGCM a local RPA is used only once, namely, as to define an initial condition for the dynamical evolution of the correlations during the reaction. In this paper we are going to consider the particular case of the TDGCM for harmonic (small amplitude) motion in the correlation channels. Of course the TDGCM model can also be

presented without making the harmonic assumption which is usually justified if the amplitude of the correlations is small. In the general case we have a large amplitude theory of the dynamical evolution of correlations perpendicular to the path. This is not an eigenvalue problem as in stationary RPA or GCM, but an initial value problem. The TDGCM aims to determine the time evolution of an initially given oscillation (orthogonal to a TDHF trajectory) and the corresponding ground state correlations. The objective is to find an equation of motion for $|\phi_q(t)\rangle$ and $f(q,t)$ in Eq. (5·1) by varying $\langle\psi(t)|H-i(\partial/\partial t)|\psi(t)\rangle$ with respect to f and $|\phi\rangle$. This variation requires some simplifications which are fulfilled in the Gaussian overlap approximation (GOA)

$$\langle\phi_q(t)|\phi_{q'}(t)\rangle=\exp\left\{-\frac{\lambda(\bar{q},t)}{2}(q-q')^2\right\} \tag{5·2}$$

with $\bar{q}=\frac{1}{2}(q+q')$ and

$$\lambda(q,t)=\langle\phi_q(t)|\frac{\overleftarrow{\partial}}{\partial q}\frac{\vec{\partial}}{\partial q}|\phi_q(t)\rangle\,. \tag{5·3}$$

The GOA allows to define a collective wave function

$$g(q,t)=\int dq'\left(\frac{\lambda(q,t)}{\pi}\right)^{1/4}\exp\left\{-\frac{\lambda(q,t)}{2}(q-q')^2\right\}f(q',t) \tag{5·4}$$

such that for any operator $\hat{A}$ one obtains

$$\begin{aligned}\langle\psi(t)|\hat{A}|\psi(t)\rangle=\int dq g^*(q,t)\Big\{&\langle\phi_q(t)|A|\phi_q(t)\rangle\\&-\frac{1}{4\lambda}\frac{\partial^2}{\partial q^2}\langle\phi_q(t)|A|\phi_q(t)\rangle\\&+:\left(-i\frac{\partial}{\partial q}\right)\langle\phi_q(t)|\frac{\overleftarrow{\partial}}{\partial q}A-A\frac{\vec{\partial}}{\partial q}|\phi_q(t)\rangle/\lambda:\\&+:\left(-\frac{\partial^2}{\partial q^2}-\frac{\lambda}{2}\right)\langle\phi_q(t)|\frac{\overleftarrow{\partial}^2}{\partial q^2}A-2\frac{\overleftarrow{\partial}}{\partial q}A\frac{\vec{\partial}}{\partial q}+A\frac{\vec{\partial}^2}{\partial q^2}|\phi_q(t)\rangle:\Big\}g(q,t)\,.\end{aligned} \tag{5·5}$$

If one inserts for $\hat{A}$ the $H-i(\partial/\partial t)$ and varies with respect to $|\phi_q(t)\rangle$, one obtains in lowest order

$$\left(H_{\rm ph}-i\frac{\partial}{\partial t}\right)|\phi_q(t)\rangle=0\,, \tag{5·6}$$

where $H_{\rm ph}$ is the 1p-1h part of the total Hamiltonian with respect to $|\phi_q(t)\rangle$. This is exactly the time dependent Hartree-Fock equation for each $|\phi_q\rangle$. The

variation with regard to $g(q)$ yields an equation for $g(q, t)$ which describes the time evolution of the superposition function $g(q, t)$ or $f(q, t)$. In case of harmonic motions in q orthogonal to the TDHF trajectories the $g(q, t)$ can be written as

$$g(q, t) = \exp\left\{-\frac{q^2}{2\alpha(t)}\right\} \tag{5·7}$$

with

$$i\frac{\partial}{\partial t}\alpha(t) = -\frac{1}{2\lambda(0, t)}\langle\phi_0(t)|\vec{\delta}_q{}^2 H - H\vec{\delta}_q{}^2|\phi_0(t)\rangle/\lambda(0, t), \tag{5·8}$$

where all values are to be taken at $q=0$. The spreading width $\Delta^2 A$ of a one-body operator can also be given very simply as

$$\begin{aligned}\langle\psi|\Delta^2 A|\psi\rangle = &\langle\phi_0|\Delta^2 A|\phi_0\rangle \\ &+\frac{1}{2}\left(\frac{\alpha\alpha^*}{\alpha_r}-\mu\right)|\langle\phi_0|\vec{\delta}_q A + A\vec{\delta}_q|\phi_0\rangle|^2 \\ &+\frac{i\alpha_i}{\alpha_r}\mu\langle\phi_0|\vec{\delta}_q A + A\vec{\delta}_q|\phi_0\rangle\langle\phi_0|\vec{\delta}_q A - A\vec{\delta}_q|\phi_0\rangle \\ &+\frac{1}{2}\left(\frac{1}{\alpha_r}-\frac{1}{\mu}\right)\mu^2|\langle\phi_0|\vec{\delta}_q A - A\vec{\delta}_q|\phi_0\rangle|^2 .\end{aligned} \tag{5·9}$$

This can be evaluated straightforwardly after performing two successive TDHF calculations with varying δq-initial conditions, and after solving the differential equations for $\alpha(t)$.

Altogether we see that in the harmonic approximation all information on $|\psi(t)\rangle$ is carried by the three quantities $|\phi_0(t)\rangle$, $\partial/\partial q|\phi_0(t)\rangle$ and $\alpha(t)$. See the complete set of Eqs. (5·6)$\sim$(5·9). In practice we handle the $\partial/\partial q|\phi_0(t)\rangle$ as finite difference $\partial/\partial q|\phi_0(t)\rangle = (|\phi_{\delta q}(t)\rangle - |\phi_0(t)\rangle)/\delta q$. Thus it remains to propagate two neighboured TDHF trajectories $|\phi_0(t)\rangle$ and $|\phi_{\delta q}(t)\rangle$ and to work out additionally the time evolution of the width $\alpha(t)$ by solving Eq. (5·8). Obviously this procedure can easily be implemented into any existing TDHF code. The extra expense of TDGCM consists mainly in carrying TDHF twice. The numerical applicability and the relevance of the TDGCM theory has been checked by means of a one-dimensional TDHF code with quartet symmetry and using the $\alpha+\alpha$-system. The force used corresponds to a single particle Hamiltonian of the form

$$h[\rho] = -\frac{\hbar^2}{2m}\frac{d^2}{dx^2} + \frac{V_0}{\sqrt{\pi}E}\int dx' \exp\left\{-\frac{(x-x')}{\sigma}\right\}\rho(x') + t_3\rho^2(x)$$

with $V_0 = -50$ MeV, $\sigma = 2$ fm, $t_3 = 88$ MeV fm^3. The TDHF solutions show fusion up to an incoming momentum of $p = 0.28$ fm^{-1}.

Since we have only one spatial coordinate, there are only a few collective modes, associated to q, to be excited. There are basically seven modes possible whose characteristics are given in Fig. 18. Corresponding to the three modes, we have six observables. We consider the following three of them:

$$\hat{P}_{\mathrm{rel}} = \int_0^\infty dx \hat{j}(x) - \int_{-\infty}^0 dx \hat{j}(x),$$

$$\hat{R}_+^2 = \int_0^\infty dx\, x^2 \hat{\rho}(x) + \int_{-\infty}^0 dx\, x^2 \hat{\rho}(x),$$

$$\hat{R}_-^2 = \int_0^\infty dx\, x^2 \hat{\rho}(x) - \int_{-\infty}^0 dx\, x^2 \hat{\rho}(x)$$

and in addition the difference in particle number

$$\hat{N}_{\mathrm{rel}} = \int_0^\infty dx \hat{\rho}(x) - \int_{-\infty}^0 dx \hat{\rho}(x).$$

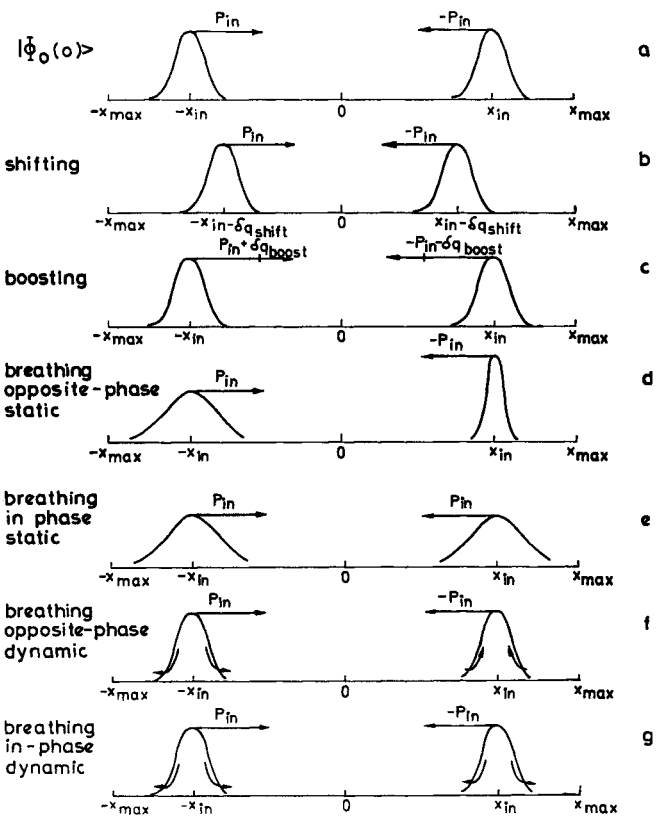

Fig. 18. The various initial configurations in TDGCM used to start the initial TDHF trajectories. The (a) combined with one of the other configurations defines the RPA correlations to be considered.

These are the operators to be inserted in place of $\hat{A}$ in Eq. (5·5).

A simple numerical test of the theory is the study of an RPA vibration within one single cluster. We take $|\phi_0(t)\rangle = |\phi_0\rangle$ as the stationary Hartree-Fock solution and for $|\phi_{\delta q}(0)\rangle$ we start with a static compression of the H.F. state. The results are shown in Fig. 19. We observe harmonic oscillations for the input quantities $(2\mu)^{-1} = \langle\phi_0|\tilde{\delta}_q\vec{\partial}_q|\phi_0\rangle$ and $\mathrm{Im}(\alpha)$. For the "measurement", namely, the spreading width of $\Delta^2\hat{R}^2$ we have three cases: First, the pure TDHF state (dotted line) produces a constant but too small width. Second, we have initialized TDGCM with the pure TDHF state (dashed line); as a result the correlated ground state oscillates about the true RPA width. Third, we start TDGCM with the true RPA width (full line) and indeed we obtain a nice straight line over many periods of oscillation. This proves the physical relevance and the numerical stability of the TDGCM.

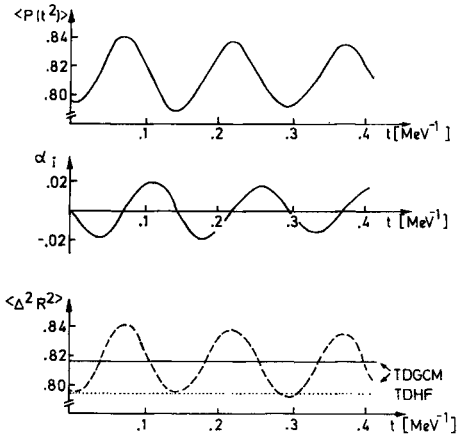

Fig. 19. The spreading width of the rms-radius of a single fragment in dependence of the time. The TDHF indicates the static HF solution made time dependent by a triaxial phase factor. The TDGCM solutions are once started with the TDHF width (oscillating curve) and once with the correct RPA-width (straight line). Although the curves look schematic, they are explicitly calculated.

As we have seen in Fig. 18, we can initiate each mode in various phases, statically or dynamically as any phase in between. If we start the TDGCM initial condition in different phases, the clusters will reach the interaction region in different stages of the internal oscillations and thus the coupling will behave quite differently. An obvious solution of this problem would be to average over many phases. In fact, it turns out that it is sufficient to use a two channel TDGCM where both channels are initiated into the same mode but with phases differing by $\pi/2$.

Now, having shown the numerical reliability of TDGCM and knowing how to assure phase stability, we can evaluate every combination of initialization and measurement. The results are given, for various impact momenta p_{in}, in Table I and the values are extracted from $|\psi(t)\rangle$ immediately after the separation of the ions. First, we observe strong contributions from the collective correlations to the spreading widths. Moreover we see that the dominant contribution always comes from that initial mode which is related

to the measurement; this feature could be called "channel-memory". The cross-channel contributions are much smaller. One cannot exclude that many of them may add up to another substantial enhancement, but a larger manifold of channels can only be treated statistically.

In Table I we see also that the correlation effects are the strongest for low momenta, near the fusion window at $p_{in}=0.28\,fm^{-1}$, and tend to decrease for higher impact momenta. In Fig. 20 we have plotted the TDGCM result for the spreading width of the internal excitation energy E^* (after reaction) as a function of p_{in}. We see that the correlations indeed produce a significant enhancement of $\Delta^2 E^*$, particularly for low p_{in} near the fusion window. For larger p_{in} the contribution decreases but seems to level off at a ratio of about 2, leaving perphaps a strong effect also for fast processes.

The increase of the energy width by an order of magnitude in TDGCM compared to TDHF is a remarkable result. Although the present calculations

Table I. The spreading width of various measuring operators is given for TDHF and for a couple of explicitly considered correlated time dependent states treated by means of TDGCM. The TDGCM is initialized using the TDHF width. One notices that for a given measuring operator only the correlations of the corresponding mode contribute essentially. The important point is that this correspondence is not destroyed in the interaction area. Apparently the treated RPA correlations have in some cases a substantial effect on the spreading width, which, however, decreases with increasing impact momentum, or with decreasing interaction time.

Initialization	Measurement			
	$\Delta^2 p_{rel}$ [fm^{-2}]	$\Delta^2 R_+^2$ [fm^4]	$\Delta^2 R_-^2$ [fm^4]	$\Delta^2 N_{rel}$
$p_{in}=0.30\,fm^{-1}$ TDGCM:				
shift+boost	2.40	18.03	10.01	0.51
breathing (+)	0.42	35.60	10.01	0.51
breathing (−)	0.29	16.51	13.14	0.52
TDHF	0.28	16.50	10.00	0.50
$p_{in}=0.35\,fm^{-1}$ TDGCM:				
shift+boost	0.88	7.81	6.43	0.36
breathing (+)	0.31	9.60	6.42	0.36
breathing (−)	0.30	5.74	7.86	0.33
TDHF	0.29	5.73	6.42	0.36
$p_{in}=0.40\,fm^{-1}$ TDGCM:				
shift+boost	0.63	5.79	4.84	0.24
breathing (+)	0.31	6.04	4.84	0.24
breathing (−)	0.30	4.86	5.02	0.24
TDHF	0.30	4.85	4.84	0.24

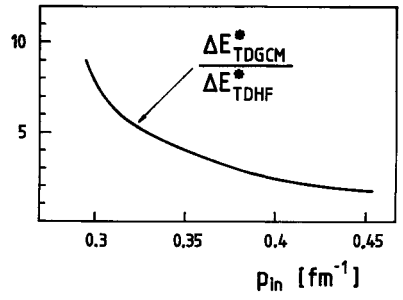

Fig. 20. The ratio of the spreading of the internal excitation energy of the fragments evaluated by TDGCM to the one evaluated by TDHF. One realizes a remarkable increase up to an order of magnitude due to the correlations considered in TDHF. The system fuses for relative momenta smaller than 0.28 fm^{-1}.

are only one dimensional and we have considered only a few modes, it shows that the sort of correlations treated in TDGCM is simply necessary for a correct description of the width of one-body operators. These correlations are actually created by a coherent superposition of different mean fields associated to the collective coordinate q. By a simple argument of Feldmeier[5] it can be shown that particularly in the case of the particle number width in a HI reaction such a superposition is the preferable mechanism to enlarge the TDHF width, compared to the inclusion of collision terms. Figure 21 illustrates this. If by the use of a collision term a particle is transferred from one ion to the other, it is bound to occupy a high-lying state since the potential well is not changed. If we, on the other hand, allow a change of the potential well as it is done in TDGCM by a superposition of many of them, then the additional particle can occupy a lower-lying state in a broader potential. Hence the superposition is energetically favoured. This corresponds also to the findings of Wolschin.[5] Thus the present mechanism described in TDGCM is probably indispensable for a correct description of widths and preferable to inclusion of collision terms.

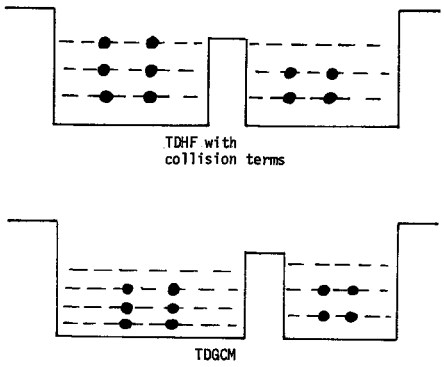

Fig. 21. Schematic picture to illustrate the difference between TDHF including collision terms and TDGCM in case of particle transfer relevant for the description of particle number widths in deep inelastic HI reactions.

§ 6. Summary

The present lecture series can be summarized by a few qualitative state-

ments:

1) The basic success of TDHF for heavy ion collisions consists in providing a good insight into the geometry of shapes involved in a HI reaction, in describing well the energy flow from the entrance channel to internal excitatations (heat) for deep inelastic reactions and also for fusion events. Furthermore, the time evolution of one-body operators turns out to be well described.

2) The disadvantage of TDHF consists in the difficulty to extract quantummechanical information from it. There are no ways to describe barrier penetration phenomena in low energy fusion events. TDHF does not give phase shifts or even clearly defined reaction channels. TDHF gives a continuum of vibrational excitations rather than a discrete spectrum.

3) Adiabatic approaches are very useful in describing barrier penetrations and vibrational states. As shown in the quantized ATDHF approach, the old problem of quantization is simply solved by now and also the collective path can explicitly be evaluated numerically with fully three-dimensional coordinate and momentum space techniques. It seems to be that the forces used have to be improved in order to reproduce correctly the experimental fusion data.

4) The functional integral approaches are conceptually a progress since they provide means to extract quantummechanical information from TDHF without explicitly making the adiabatic approximation. They also can be used to formulate a complete reaction theory. For bound states they result in a multitude of periodic TDHF orbits and a quantization condition. Unfortunately numerical calculations in realistic systems are missing and do not seem to be available in the near future.

5) There is a strong relationship between PIA and quantized ATDHF. The adiabatic approximation incorporated in PIA yields the ATDHF equation and the corresponding collective path, which means that the ATDHF path is a well defined approximation to the multitude of period TDHF trajectories. The semiclassical approximate solution of the quantized ATDHF collective Hamiltonian reproduces the quantization condition of PIA also when fluctuations are taken into account.

6) If one sticks to the semiclassical nature of TDHF and is interested in inclusive cross sections, then correlations due to collision terms and due to RPA vibrations on top of TDHF go beyond the TDHF approach. In the first sort of approaches excited single particle levels of the TDHF like potential well are fractionally occupied. In the second case, i.e., time dependent GCM (TDGCM), several Slater determinants associated to different mean fields are superimposed. Actual one-dimensional calculations show that the latter theory is able to explain the large widths of one-body operators not reproduced by TDHF. This is particularly relevant for the description of

particle number fluctuation in HI reactions, which is probably due to RPA correlations and not due to statistical two-body collisions. However, calculations for this particular example are missing yet since they are bound to involve pairing correlations. Calculations in more than one dimension, allowing also for finite impact parameters, are also missing.

References

1) P. Bonche, S. Koonin and J. Negele, Phys. Rev. **C13** (1976), 1226.
2) R. Y. Cusson, J. A. Maruhn and W. A. Meldner, Phys. Rev. **C18** (1978), 2589.
3) K. T. R. Davies, K. R. Sandhya-Devi and M. R. Strayer, Phys. Rev. **C20** (1978), 1372.
4) J. W. Negele, Rev. Mod. Phys. **54** (1982), 913.
5) *Proc. Int. Meeting at Bad Honnef, June 7~11, 1982*, ed. K. Goeke and P. -G. Reinhard, *Lecture Notes in Physics* (Springer-Verlag, 1982).
6) G. Holzwarth and T. Yukawa, Nucl. Phys. **A219** (1974), 125.
7) D. J. Rowe and R. Bassermann, Can. J. Phys. **54** (1976), 1941.
8) T. Marumori, Prog. Theor. Phys. **57** (1977), 112.
9) F. Villars, Nucl. Phys. **A285** (1977), 269.
10) K. Goeke and P.-G. Reinhard, Ann. of Phys. **112** (1978), 328.
11) M. Baranger and M. Véneroni, Ann. of Phys. **114** (1978), 123.
12) P.-G. Reinhard and K. Goeke, Nucl. Phys. **A312** (1978), 121.
13) P.-G. Reinhard and K. Goeke, Phys. Rev. **C20** (1979), 1546.
14) P.-G. Reinhard, J. A. Maruhn and K. Goeke, Phys. Rev. Letters **44** (1980), 1740.
15) H. Reinhardt, Nucl. Phys. **A346** (1980), 1.
16) S. Levit, J. Negele and Z. Paltiel, Phys. Rev. **C21** (1980), 1603.
17) H. Kuratsuji and T. Suzuki, Phys. Letters **92B** (1980), 19.
18) J. P. Blaizot and M. Orland, J. de Phys. **41** (1980), L53.
19) P.-G. Reinhard, K. Goeke and R. Y. Cusson, Z. Phys. **A295** (1980), 45.
20) P.-G. Reinhard, R. Y. Cusson and K. Goeke, *Time Evolution of Coherent Ground State Correlations and the TDHF Approach*, to be published.
21) C. Y. Wong and H. H. Tang, Phys. Rev. Letters **40** (1978), 1070.
22) H. S. Köhler, Nucl. Phys. **A343** (1980), 315.
23) P. Grangé, H. A. Weidenmüller and G. Wolschin, Ann. of Phys. **136** (1981), 190.
24) R. Balian and M. Véneroni, Ann. of Phys. **135** (1981), 270.
25) S. Ayik, Z. Phys. **A298** (1980), 83.
26) A. F. R. de Toledo Piza, see Ref. 5).
27) H. C. Pauli, see Ref. 5).
28) K. Goeke, P.-G. Reinhard and D. J. Rowe, Nucl. Phys. **A359** (1981), 408.
29) D. J. Rowe and A. Ryman, *Valleys and Fall Lines on a Riemannian Manifold*, Preprint Toronto, to be published.
30) H. Flocard, P. H. Heenen and D. Vautherin, Nucl. Phys. **A339** (1980), 336.
31) K. K. Kan, J. J. Griffin, P. C. Lichtner and M. Dworzecka, Nucl. Phys. **A332** (1979), 109.
32) K. Goeke, P.-G. Reinhard and H. Reinhardt, Nucl. Phys. **A378** (1982), 474.
33) H. Feldmeier, see Ref. 5).
34) G. Wolschin, see Ref. 5).
35) K. Goeke and P.-G. Reinhard, Ann. of Phys. **124** (1980), 249.